Cooperative Mercury Motion in the Ionic Conductor Cu_2HgI_4

Damjan Pelc, Igor Marković, and Miroslav Požek

Department of Physics, Faculty of Science, University of Zagreb, Bijenička 32, HR-10000, Zagreb, Croatia

(Received 5 January 2012; published 29 August 2012)

We present the observation of glasslike dynamic correlations of mobile mercury ions in the ionic conductor Cu_2HgI_4, detected in both NMR and nonlinear conductivity experiments. The results show that dynamic cooperativity appears in systems seemingly unrelated to glassy and soft arrested materials. A simple kinetic two-component model is proposed, which seems to provide a good description of the cooperative ionic dynamics.

DOI: 10.1103/PhysRevLett.109.095902 PACS numbers: 66.30.H−, 61.43.−j, 76.60.−k, 81.05.Kf

In glass-forming materials, particles increasingly move together as the glass transition is approached [1,2]. Such cooperativity is also found in other arrested systems [3–6] and seems to be intimately connected to the slow dynamics. Here, we report on the observation of large-scale dynamic correlations in a distinctly nonglassy system—the conductive phase of the ionic conductor Cu_2HgI_4. Using carefully designed nuclear magnetic resonance experiments, we prove that mercury ions are the main contributors to conduction (establishing Cu_2HgI_4 as the first known mercury conductor) and show that mercury diffusion is anomalous. These results urge for a more detailed examination of ionic motion. Therefore, nonlinear conductivity measurements are used as a probe for dynamical heterogeneity, revealing a characteristic correlation time scale. To explain the cooperativity we propose a simple model related to previous work on glasses [7,8], with two essential ingredients—disorder and existence of two kinds of particles, slow (copper) and fast (mercury). We compare the results with recent studies of arrested and glass-forming materials [2,3], thus establishing an unexpected connection between seemingly different fields.

Cu_2HgI_4 used in experiments was in powder form, synthetized according to standard procedure [9]. X-ray diffraction at 300 K showed no appreciable contamination with iodides, and all applied techniques (NMR, DSC, conductivity) saw a sharp transition at $T_c = 344.7$ K, providing further evidence of phase purity. Free induction decays were used to record NMR line shapes, while a recovery sequence was employed in the ^{63}Cu relaxation measurements. Conductivity was measured in a two-contact cylindrical cell with graphite electrodes, using a low distortion voltage source and lock-in amplifier. At all temperatures, sample resistance was above 1 MΩ. Low frequency (7 Hz) conductivity agrees quantitatively with previously published values [10,11]. The third harmonic current j_3 provided nonlinear conductivity; the heating contribution to j_3 was estimated to be small due to large sample resistance, and more importantly, uniform over the employed frequency range (linear conductivity is not peaked). Instrumental harmonic distortion effects were also negligible between ∼10 Hz and ∼20 kHz. All measurements were reproducible after several temperature cycles across T_c.

Before studying cooperative ionic motion in Cu_2HgI_4, we must identify the charge carriers and nature of the insulator-conductor transition at T_c. Ever since the discovery of ionic conduction in Cu_2HgI_4 [12], it has remained unclear which ion species predominantly carries current in the conducting phase above T_c [11,13]. Here we obtain direct proof of mercury motion from NMR experiments—a substantial motional narrowing of the mercury line in the conductive phase [Fig. 1(a)]. In contrast, the copper line is broadened, indicating quasistatic disorder. This suggests that the transition is not melting of the copper sublattice (unlike the related CuI [14]), but rather an order-disorder transition [15] with the copper ions remaining virtually static. Mercury motion is then enhanced in the changed energy landscape above T_c. Slow copper diffusion and disorder are essential for explaining mercury dynamic cooperativity, so we perform NMR line shape and relaxation measurements on copper to provide a microscopic picture of the transition.

The structure of Cu_2HgI_4 in the ordered phase below T_c contains 8 tetrahedral positions per unit cell, with only 3 occupied by copper or mercury [13]. Thus one expects that a relatively small activation energy is necessary to create point defects by moving ions from ''regular'' to normally empty tetrahedral positions. NMR enables us to follow these motions in an ion-specific way, and observe how they lead to a transition to the disordered phase. Naturally abundant copper nuclei are quadrupolar and thus sensitive to electric field gradients (EFGs) present in the material. This is already obvious in the NMR line shapes—the local environment of copper ions doesn't have cubic symmetry, leading to a quadrupolar splitting of the line. While all Cu^+ which are on regular sites have roughly the same local environment, ions on normally vacant sites (defects) experience much larger EFGs and their NMR lines are substantially shifted and broadened [16]. The signal from defects thus contributes as a low, broad background easily separable from the narrow line of

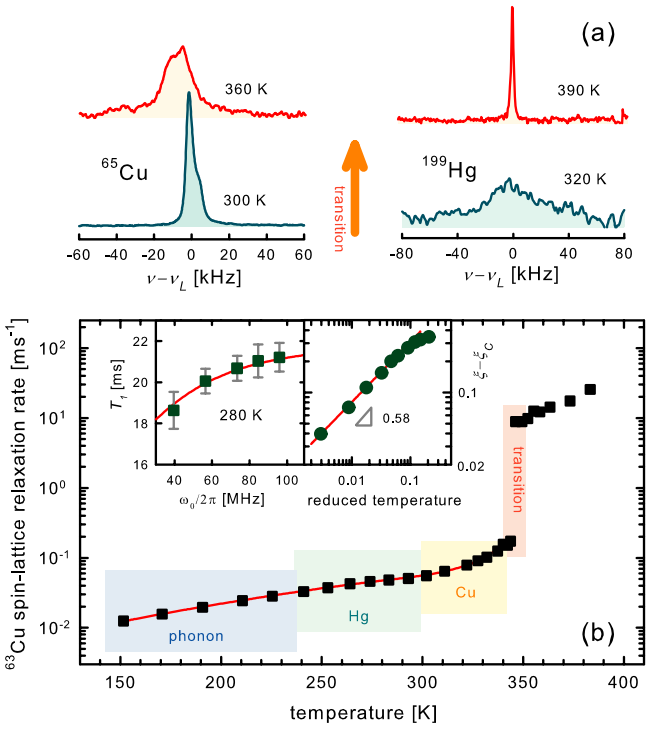

FIG. 1 (color online). (a) NMR lines of copper and mercury, below and above T_c. Frequency is relative to Larmor frequencies, 145.6 MHz for ^{65}Cu and 91.2 MHz for ^{199}Hg. Pulse excitation width is ~150 kHz. Copper lines are normalized to have the same integrals, while the low-temperature mercury line is multiplied by 10 after normalization. Significant motional narrowing is observed for mercury above T_c. (b) Spin-lattice relaxation measurements for ^{63}Cu. Left inset is frequency dependence at 280 K. Lines are fits obtained from a superposition of phonon and two defect diffusion processes (mercury and copper). Temperature ranges where each of the processes comes into play are indicated. Right inset is order parameter in dependence on reduced temperature.

"regular" Cu^+. The integral of the narrow line can be used to obtain the relative number of defects. This number is expected to grow anomalously fast close to an order-disorder transition, as is indeed observed. One can even see power-law behavior close to T_c, described reasonably well with a mean-field approach. We define an order parameter $\xi = (n_l - n_v)/(n_l + n_v)$, with n_l and n_v the number of regular copper atoms and copper defects, respectively. The transition being first order, ξ drops abruptly to zero above T_c. A Landau expansion yields $\xi - \xi_c \sim \epsilon^\beta$ close to T_c, with ξ_c the order parameter at T_c, $\epsilon = (T_c - T)/T_c$ the reduced temperature and β the critical exponent: $\beta = 1/2$, comparing well with the experimental value of 0.58 (Fig. 1(b) right inset). At T_c the lattice reorganizes and the distinction between "defects" and "regular" copper ions is lost, as all Cu^+ positions are equally probable [17]. However, no motional narrowing of the copper line is observed above T_c. Instead, the line broadens due to larger EFGs caused by electrostatic disorder.

To learn more about defect dynamics we measure copper spin-lattice relaxation [Fig. 1(b)]. Diffusing defects create fluctuating EFGs, which influence the relaxation. In addition to a conventional Raman phonon mechanism [18], we observe effects of both mercury and copper defect diffusion on the relaxation rate below T_c. The contribution from one defect type is [14,16]

$$\left.\frac{1}{T_1}\right|_{\text{def}} \approx \delta\omega_Q^2 n_v(T) \frac{\tau_h(T)}{1 + [\omega_L \tau_h(T)]^2} \tag{1}$$

with $\delta\omega_Q$ a temperature-independent quadrupolar coupling constant, τ_h hopping time and ω_L Larmor frequency. The hopping process is thermally activated [19], with $\tau_h = \tau_0 e^{E_h/kT}$, where $1/\tau_0$ is the attempt frequency and E_h the hopping activation energy. The numbers of defects also follow Arrhenius-type laws except close to T_c. Combining the temperature and frequency dependences of the relaxation rate, with attempt frequencies estimated from Raman spectroscopy [20], we obtain E_h for both copper and mercury defects [21]. The values are 4900 ± 100 K and 2220 ± 50 K for copper and mercury, respectively. Thus already below T_c mercury has a significantly lower hopping activation energy than copper. Microscopic reasons are as of yet unclear.

Above T_c the mercury diffusion rate increases for an order of magnitude and the ^{199}Hg line becomes motionally narrowed. The line shape is well fitted by a Lorentzian curve and the hopping time can be extracted from the linewidth using $\Delta\omega = (\Delta\omega_0)^2\tau_h$, where $\Delta\omega_0$ is the static linewidth (below T_c). The simple formula is valid for $\Delta\omega_0\tau_h \ll 1$, so we have taken into account corrections for finite τ_h where necessary [22]. Employing the Einstein relation for mobility, we can try to calculate the conductivity from extracted hopping times:

$$\sigma_0 = \frac{2e^2 n}{kT}\frac{L^2}{\tau_h}, \tag{2}$$

where $2e$ is the charge of Hg^{2+} ions, n their number density ($\sim 5 \times 10^{21}$ cm^{-3}) and L a hopping distance of the order of the interatomic spacing (~ 1 Å). If we now take this conductivity and compare it to the measured dc values, we observe the first sign of anomalous behavior: in a region ~30 K above T_c, σ_0 is significantly larger than σ_{dc} [Fig. 2(a)]. Thus relation (2), valid for simple stochastic motion of ions, doesn't correctly predict the long-time transport. One may ask if this is due to the existence of some new, intermediate time scale above $\tau_h \sim 1$ μs where motional correlations arise, or just well-known short range correlation effects quantified with the Haven ratio [23]. To resolve the question, we measure the nonlinear conductivity $\sigma_3(\omega)$, defined by $j = \sigma_1 E + \sigma_3 E^3 + \ldots$, in dependence on frequency ω [Fig. 2(b)]. Although dynamical correlation effects often bear small influence on linear response, they are intimately related to nonlinear susceptibilities. A quantitative measure is the four-point

correlation function [24–26], $C_4(\mathbf{y},t)=\langle f(\mathbf{x},0)f(\mathbf{x}+\mathbf{r},t)\times f(\mathbf{x}+\mathbf{y},0)f(\mathbf{x}+\mathbf{y}+\mathbf{r},t)\rangle_{\mathbf{x}}$ (with f a suitable dynamic parameter, e.g., intermediate scattering function), representing the correlation of time changes at different points in space. Thus, if many ions move synchronously on a characteristic time scale τ_{corr}, $C_4(\mathbf{y}, t)$ will have a peak at τ_{corr}. Generalized fluctuation-dissipation theorems connect χ_4, the spatial integral of C_4, with the corresponding nonlinear susceptibility [24], making dynamical correlations measurable. In contrast to the case of a dielectric (or magnetic) material, where one measures the response of dipoles to an external field, we detect the response of mobile charges, and the natural response function is σ_3 instead of the susceptibility χ_3. A lot of activity is currently aimed at modeling dynamical heterogeneity in soft and glassy systems [27], but experimental data are still scarce—the first report on nonlinear susceptibility of a glass-former (glycerol) only appeared recently [2]. Here, we see similar effects, but in a rather unexpected material. Characteristic correlation time scales are revealed through peaks in $\sigma_3(\omega)$ at frequencies $\omega\tau_{\mathrm{corr}}\sim 1$, and the relative number of correlated ions, N_{corr}, can be estimated from integrals of the peaks [Fig. 2(a)]. In our work we focused on σ_3 as it is sensitive to correlated motion; we note, however, that the new correlation time scale also affects the linear conductivity $\sigma_1(\omega)$. A shoulderlike feature is visible at the frequency $1/\tau_{\mathrm{corr}}$ in the frequency spectrum of σ_1: this strengthens the analogy with supercooled liquids, where, similarly, the peak of the nonlinear response occurs close to the characteristic relaxation frequency visible in linear response.

Except very close to the transition, τ_{corr} is substantially longer than the mercury hopping time τ_h. Thus a simplistic conduction model can be used to explain the discrepancy between σ_0 and σ_{dc}. We assume that mercury ions move vigorously most of the time, but sometimes get constrained to small volumes. NMR lines of these ions are broad and do not contribute to the principal narrow line. Occasionally several trapped ions arrange favorably, and leave the "trap" together. Thus, the effective number of charge carriers is diminished and the characteristic correlation time scale appears. This is essentially a "cooperatively rearranging regions" (CRR) scenario, well known in glass science [8,28]. A similar mechanism was also proposed for colloidal gel relaxations [3], and seems to offer a good phenomenological explanation of our data. Contrary to glass-forming liquids, where N_{corr} has no effect on σ_{dc}, here the correlations influence it. We obtain direct experimental evidence for this model from a different NMR experiment on mercury—stimulated spin echo (SSE) measurements (Fig. 3). Moving spins experience much smaller average local fields than trapped ones, leading to a difference in spin decoherence times. This can be exploited to selectively excite and detect only ions moving at a given moment. The SSE sequence [29] is perfectly suited for such an experiment [30]. After correcting for spin-lattice

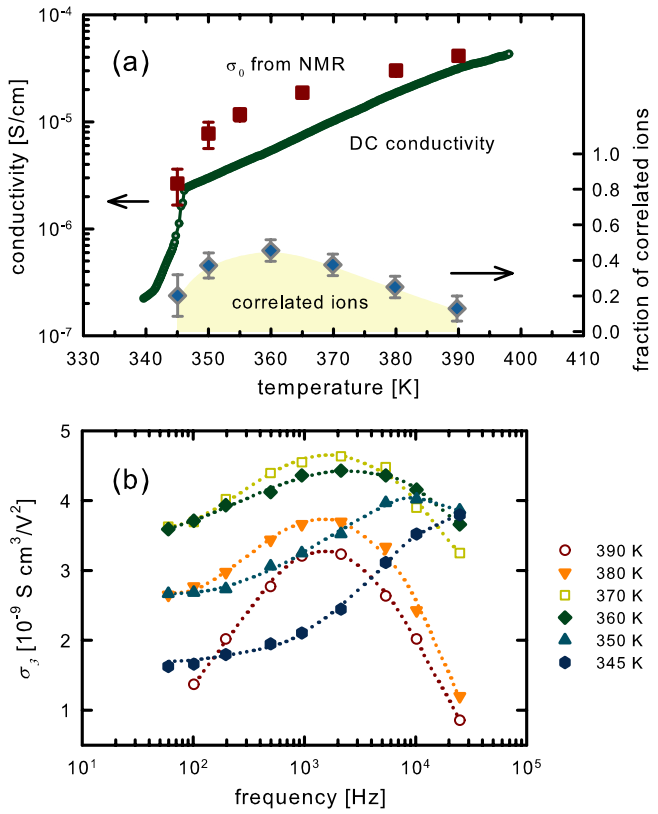

FIG. 2 (color online). (a) dc conductivity (circles) is smaller than conductivity predicted from mercury NMR (squares), indicating anomalous behavior. The discrepancy between conductivities closely follows the number of correlated ions (diamonds, estimated from nonlinear conductivity and NMR) (b) nonlinear conductivity in dependence on frequency. Peaks clearly show the existence of a cooperativity time scale. Nonlinear response below T_c is negligible. Lines are guides to the eye.

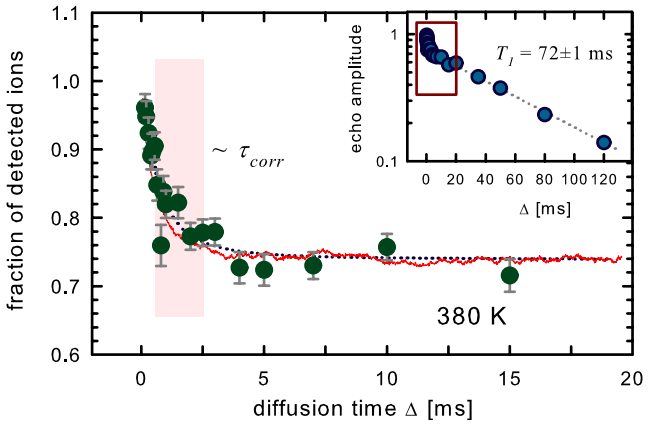

FIG. 3 (color online). Stimulated spin echo NMR measurements at 380 K, giving evidence of mercury ion trapping at the characteristic time scale τ_{corr}. Inset is raw measurement, the square denoting the zoomed-in segment where dynamic trapping effects are visible. Main graph is compensated for spin-lattice relaxation, showing only the correlation contribution. Full line is from simulation, and the dotted line a stretched exponential fit.

relaxation, we can directly observe how, of all ions moving at the time of excitation, a sizeable fraction becomes trapped after a time $\Delta \sim \tau_{\mathrm{corr}}$ (Fig. 3). This experiment provides an absolute scale for N_{corr}, and we can make a comparison with the difference between σ_0 and σ_{dc} [Fig. 2(a)]. The agreement is gratifying, both in absolute scale and temperature dependence, implying that the difference can be attributed to a diminished effective number of carriers, confirming the phenomenological model.

However, microscopic questions remain: what causes confinement, and how are correlated jumps performed? To answer them, we propose a very simple mechanism, related to investigations of spin glasses (essentialy a limiting case of the Edwards-Anderson Hamiltonian with diffusion [7,31]). Aside from disorder, the basic requirement is the existence of two kinds of atoms in the material, with different diffusion coefficients, and short-range interactions. In Cu_2HgI_4 this is realized with copper and mercury, on a fixed iodine background. If we take low-temperature activation energies to be representative, we can conclude that mercury diffuses 10^3 to 10^4 times faster than copper in the interesting temperature range where correlations appear. As slow copper ions move around, they occasionally form compartments with several trapped mercury ions inside. The compartments can then ''open'' due to cation rearrangement—once a path is open, many fast mercury ions use it sequentially to empty the compartment. Such behavior is indeed observed in a two-dimensional random walk simulation. Simulations were run on a square lattice with periodic boundary conditions and initially randomly placed ions. In every step the mercury ions moved in random (allowed) directions, while the copper ions moved with a certain probability D^* (which is essentially the ratio of copper and mercury diffusion coefficients). In the course of simulation large mercury ''islands'' form and dissolve (Fig. 4, inset). To calculate the four-point correlation function χ_4, we used the persistence function [32], defined as $n_{\mathbf{r}}(t_0) = 1$ if nothing has happened on site $\mathbf{r}$ for $t < t_0$, and $n_{\mathbf{r}}(t_0) = 0$ otherwise. χ_4 is calculated as the variance of the autocorrelation of $n_{\mathbf{r}}(t)$, evaluated at all mercury sites [33]. A characteristic correlation time scale is revealed (Fig. 4), and the curves qualitatively follow the CRR prediction [32]. The only parameters we have to set are D^* and effective particle concentration, taking care that the number of vacant sites is above the percolation threshold [34]. For realistic concentrations and D^*, correlation times become about $10^3 \tau_h$, in fair agreement with experiment. The SSE decay curve (Fig. 3) can also be predicted surprisingly well.

The model is ''minimal,'' in the sense that we obtain dynamical heterogeneity with the minimum number of assumptions. This hints at a considerable universality of such correlations. Important effects have, however, been neglected: the iodine lattice potential, short-range electrostatic correlations, electronic dynamics and phonons.

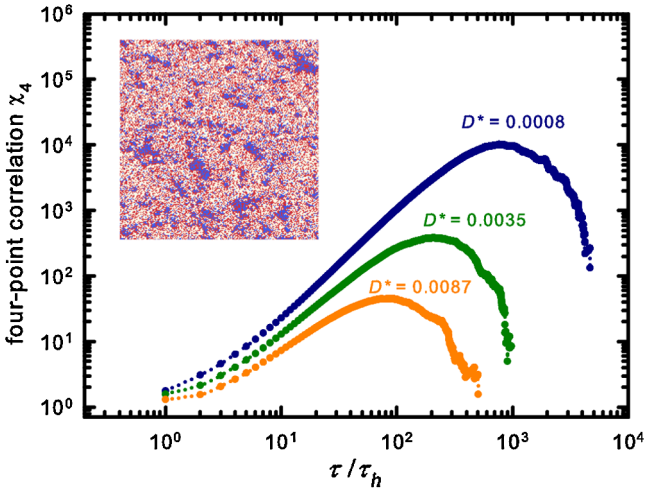

FIG. 4 (color online). Some results of the two-dimensional simulation. Inserted frame at 2000 steps shows formed mercury islands ($D^* = 0.0022$, simulation box 300×300 cells). A correlation time scale is nicely visible in the time dependence of the four-point correlation χ_4, for several D^*.

Correct temperature behavior cannot be obtained without taking them into account. In contradistinction to glass-forming materials, no slowing down of the correlated dynamics with decreasing temperature is observed in Cu_2HgI_4; we suspect that this is due to the additional periodic potential, which tends to restore an ordered state (and succeeds at T_c). Also, we believe that a full three-dimensional simulation would show similar cooperative behavior (with modified vacancy numbers due to a lower percolation threshold), but this needs to be proven. More elaborate simulations are needed to better understand these issues.

From our results we can conclude that ingredients needed for large-scale motional correlations are quite ubiquitous, so it is reasonable to believe that ionic cooperativity is important for many other systems as well. In disordered ionic conductors, it might offer a more convincing explanation of nonlinear response than standard hopping models [35], opening up new perspectives for studying ion dynamics. Even more important is the connection with arrested materials, which shows that dynamical correlations are more universal than previously thought. The observed interplay between lattice potential and dynamical heterogeneity is very interesting in itself and could provide a unique possibility for exploring the emergence of glasslike correlations.

We thank D. Cinčić and V. Stilinović for DSC and x-ray measurements and A. Dulčić, H. Buljan, S. Marion, and M. S. Grbić for helpful discussions and comments. The research leading to these results was supported by equipment financed from the European Community's Seventh Framework Programme (FP7/2007-2013) under Grant Agreement No. 229390 SOLeNeMaR and by funding from the Croatian Ministry of Science, Education and Sports through Grant No. 119-1191458-1022.

[1] *Dynamical Heterogeneities in Glasses, Colloids, and Granular Media*, edited by L. Berthier, G. Biroli, J.-P. Bouchaud, L. Cipeletti, and W. van Saarloos (Oxford University Press, New York, 2011).

[2] C. Crauste-Thibierge, C. Brun, F. Ladieu, D. L'Hote, G. Biroli, and J.-P. Bouchaud, Phys. Rev. Lett. **104**, 165703 (2010).

[3] A. Duri and L. Cipelletti, Europhys. Lett. **76**, 972 (2006).

[4] O. Dauchot, G. Marty, and G. Biroli, Phys. Rev. Lett. **95**, 265701 (2005).

[5] A. S. Keys, A. R. Abate, S. C. Glotzer and D. J. Durian, Nature Phys. **3**, 260 (2007).

[6] P. Mayer *et al.*, Phys. Rev. Lett. **93**, 115701 (2004).

[7] D. Čapeta and D. K. Sunko, Phys. Rev. B **74**, 220201(R) (2006).

[8] G. Adam and J. H. Gibbs, J. Chem. Phys. **43**, 139 (1965).

[9] Precipitation from an aqueous solution, similar to L. Suchow and P. H. Keck, J. Am. Chem. Soc. **75**, 518 (1953).

[10] L. Suchow and G. R. Pond, J. Am. Chem. Soc. **75**, 5242 (1953).

[11] S. Hull and D. A. Keen, J. Phys. Condens. Matter **12**, 3751 (2000).

[12] J. A. A. Ketelaar, Z. Kristallogr. **80**, 190 (1931).

[13] L. Eriksson, P. Wang, and P. Werner, Z. Kristallogr. **197**, 235 (1991).

[14] J. B. Boyce and B. A. Huberman, Solid State Commun. **21**, 31 (1977).

[15] M. Lumsden, M. Steinitz, and E. J. McAlduff, J. Appl. Phys. **77**, 6039 (1995).

[16] F. Reif, Phys. Rev. **100**, 1597 (1955).

[17] This is nicely seen in x-ray diffraction experiments, Ref. [13].

[18] A. Abragam, *The Principles of Nuclear Magnetism.* (Oxford University Press, New York, 2002).

[19] N. W. Ashcroft and N. D. Mermin, *Solid State Physics.* (Holt, Rinehart & Winston, New York, 1976).

[20] J. I. McOmber, D. F. Shrivera, and M. A. Ratner, J. Phys. Chem. Solids **43**, 895 (1982).

[21] See Supplemental Material at http://link.aps.org/supplemental/10.1103/PhysRevLett.109.095902 for details on the rather intricate fitting process and comments on the behavior of copper T_1 above T_c,

[22] A. Abragam (Ref. [18]). Even at the lowest temperature (345 K) the correction to a Lorentzian result is less than 20%.

[23] G. E. Murch, Solid State Ionics **7**, 177 (1982).

[24] J.-P. Bouchaud and G. Biroli, Phys. Rev. B **72**, 064204 (2005).

[25] N. Lačević, F. W. Starr, T. B. Schrøder, and S. C. Glotzer, J. Chem. Phys. **119**, 7372 (2003).

[26] J. N. Fry and P. J. E. Peebles, Astrophys. J. **221**, 19 (1978).

[27] L. Berthier and G. Biroli, Rev. Mod. Phys. **83**, 587 (2011).

[28] T. R. Kirkpatrick, D. Thirumalai and P. G. Wolynes, Phys. Rev. A **40**, 1045 (1989).

[29] E. L. Hahn, Phys. Rev. **80**, 580 (1950).

[30] See Supplemental Material at http://link.aps.org/supplemental/10.1103/PhysRevLett.109.095902 for a detailed description of the stimulated echo measurement technique.

[31] S. F. Edwards and P. W. Anderson, J. Phys. F **5**, 965 (1975).

[32] C. Toninelli, M. Wyart, L. Berthier, G. Biroli, and J.-P. Bouchaud, Phys. Rev. E **71**, 041505 (2005).

[33] The system is given an equilibration time of several (typically 10) τ_{corr}, after which the calculation of χ_4 begins.

[34] The effective number of available vacancies is possibly smaller than the geometric ratio obtained from the crystal structure, due to Coulomb repulsion between ions (some evidence for this is presented for the similar compound Ag_2HgI_4 in T. Hibma, H. U. Beyeler, and H. R. Zeller, J. Phys. C **9**, 1691 (1976).

[35] A. Heuer, S. Murugavel, and B. Roling, Phys. Rev. B **72**, 174304 (2005).